

## FIFTH INTERNATIONAL CONGRESS ON SOUND AND VIBRATION

DECEMBER 15-18, 1997  
ADELAIDE, SOUTH AUSTRALIA

*Invited Paper*

### CRACK DETECTION IN BEAMS USING STRUCTURAL INTENSITY

Christopher Norwood  
Maritime Platform Division  
AMRL-DSTO  
Melbourne, Australia

#### **ABSTRACT**

*Vibration analysis techniques have been used for crack detection for many years. Recently much of the emphasis in this area has been on the use of shifts in natural frequency as an indicator of damage. The vibration response of a structure is determined by the mass and stiffness distribution throughout the structure. In a similar manner the structural intensity or power flow in the structure is determined by the mass, stiffness and damping distributions. This paper examines the effect of a crack on the flexural power flow in a beam. Expressions for the transmission and reflection of flexural waves incident on a crack are derived. A fracture hinge representation of the crack is used and the analysis shows that at the crack there is a discontinuity in the reactive intensity. The size of the discontinuity is dependant upon the crack size and the wave number. Experimental measurements of the power flow in a simulated infinite beam with a crack are made using the wave decomposition method. These results confirm the existence of the discontinuity in the reactive intensity at the crack. The use of wave number measurements as a crack indicator was also tested experimentally and found to be superior to intensity.*

#### **INTRODUCTION**

The ideal non-destructive test should have the following features: provide a yes/no indication of defect or damage; require no baseline test; locate and quantify the defect or damage; and be easy and fast to implement. No one test technique possess all these features and there is no universal technique which is applicable to all types of structures.

Tests techniques can be divided into two classes; global tests where the entire structure is tested using a single excitation and a single response; and local tests where defects only at the location of the response measurement are detected. An example of a global test is the tapping of train wheels, while the coin tap test is a local test.

For global tests differences in frequency and damping between good and defective components are detected. The vibration response of the structure is governed by the stiffness,

damping and mass distribution throughout the structure. Damage will alter the stiffness and damping distribution, resulting in changes to the response. Local measurements rely on the entire structure being scanned and defects being detected from anomalies in the measurements. These anomalies result from local changes in the stiffness and damping.

The transmission of vibratory energy through a structure is also governed by the stiffness, damping and mass distribution throughout the structure. Measurements can be made to observe the propagation paths of the mechanical energy throughout the structure. Localised defects, such as stiffness discontinuities, cracks and damping faults will cause anomalies in the power flow patterns. These anomalies will in principal indicate the presence and location of faults.

For beam type structures the measurement of power flow due to flexural vibrations offers the possibility to detect damage by identifying local anomalies in the power flow field, or to detect changes in the local wave number at relatively low frequencies. The effect of a flexural crack on the power flow field and wave number is presented in this paper.

## MODEL FOR A CRACK IN FLEXURE

For beams in flexure the crack may be represented by a flexure hinge, as shown in Figure 1, Ju et al [1982]. The crack is replaced by a torsional spring, the stiffness of which is a function of the crack depth. Conditions of continuity and compatibility between the spring and the two beam ends then define the boundary conditions, Figure 2.

$$\begin{aligned}
 w_1(x) &= w_2(x) \Big|_{x=\beta} && \text{(displacement equality)} && ) \\
 w_1''(x) &= w_2''(x) \Big|_{x=\beta} && \text{(Moment equality)} && ) \\
 w_1'''(x) &= w_2'''(x) \Big|_{x=\beta} && \text{(shear equality)} && ) \\
 w_1'(x) + \left( \frac{EI}{k_r} \right) w_1''(x) &= w_2'(x) \Big|_{x=\beta} && \text{(stiffness relationship)} && )
 \end{aligned} \tag{1}$$

The displacements either side of the crack may be written

$$\begin{aligned}
 w_1(x) &= (A_1^+ e^{-jkx} + A_1^- e^{jkx} + B_1^- e^{kx}) \\
 w_2(x) &= (A_2^+ e^{-jkx} + B_2^+ e^{-kx})
 \end{aligned}$$

where the time dependence has been omitted for clarity. Substituting into equations (1) and cancelling the common terms

$$\begin{aligned}
 A_1^+ + A_1^- + B_1^- &= A_2^+ + B_2^+ \\
 -A_1^+ - A_1^- + B_1^- &= -A_2^+ + B_2^+ \\
 jA_1^+ - jA_1^- + B_1^- &= jA_2^+ - B_2^+ \\
 (-j - \alpha k)A_1^+ + (j - \alpha k)A_1^- + (1 + \alpha k)B_1^- &= -jA_2^+ - B_2^+
 \end{aligned} \tag{2}$$

Rearranging

$$\begin{aligned}
 A_1^+ &= -A_1^- - B_1^- + A_2^+ + B_2^+ \\
 A_1^+ &= -A_1^- + B_1^- + A_2^+ - B_2^+ \\
 A_1^+ &= A_1^- + jB_1^- + A_2^+ + jB_2^+ \\
 (j + \alpha k)A_1^+ &= (j - \alpha k)A_1^- + (1 + \alpha k)B_1^- + jA_2^+ + B_2^+
 \end{aligned} \tag{3}$$

where  $\alpha = EI/k_r$ . If  $A_1^+ = 1$  then  $A_1^-$ ,  $B_1^-$ ,  $A_2^+$  and  $B_2^+$  can be solved for

$$\begin{aligned}
A_1^- &= -\frac{2\alpha^2 k^2 + 8jak + 2j\alpha^2 k^2}{32 + 16\alpha k + 4\alpha^2 k^2} \\
B_1^- &= \frac{8\alpha k + 2\alpha^2 k^2 - 2j\alpha^2 k^2}{32 + 16\alpha k + 4\alpha^2 k^2} \\
A_2^+ &= \frac{32 + 16\alpha k + 2\alpha^2 k^2 - 8jak - 2j\alpha^2 k^2}{32 + 16\alpha k + 4\alpha^2 k^2} \\
B_2^+ &= \frac{8\alpha k + 2\alpha^2 k^2 - 2j\alpha^2 k^2}{32 + 16\alpha k + 4\alpha^2 k^2}
\end{aligned} \tag{4}$$

The power flow in a bar written in terms of the wave components is given by

$$P_T = EI\omega k^3 [ |A^+|^2 - |A^-|^2 + 2 \text{Im}(B^+ B^{*-}) ] \tag{5}$$

In the far-field, or where only one near-field component exists, then the propagating power is

$$P_{re} = EI\omega k^3 [ |A^+|^2 - |A^-|^2 ] \tag{6}$$

Substituting the wave component expressions into equation (5), because there is only one near-field term, it can be seen that the net active power on the incident side, which is the incident power minus the reflected power, is equal to the active power on the transmitted side.

The reactive power can be expressed in terms of the wave components as

$$\begin{aligned}
P_{im} = EI\omega k^3 \{ & |A^+||B^+|e^{-kx}(\cos(kx-\phi_{A+B^+})-\sin(kx-\phi_{A+B^+})) \\
& |A^+||B^-|e^{kx}(-\cos(kx-\phi_{A+B^-})-\sin(kx-\phi_{A+B^-})) \\
& |A^-||B^+|e^{-kx}(\cos(kx+\phi_{A-B^+})-\sin(kx+\phi_{A-B^+})) \\
& |A^-||B^-|e^{kx}(-\cos(kx+\phi_{A-B^-})-\sin(kx+\phi_{A-B^-})) \} \tag{7}
\end{aligned}$$

The expressions for the wave components can be substituted into equation (7) to find the reactive power. An understanding of the reactive power can be gained from two limiting cases. If  $\alpha k$  is small then  $|A_2^+| = 1$ , while  $|A_1^-|$ ,  $|B_1^-|$  and  $|B_2^+|$  are small, hence the  $|A_1^-||B_1^-|$  term in equation (7) can be ignored as second order. Also  $\phi_{A_1+B_1^-} = \phi_{A_2+B_2^+} = 0$ . This gives the reactive power on the incident side and the transmitted side as

$$P_{1im} = EI\omega k^3 |B_1^-| e^{kx} (-\cos kx - \sin kx), x \leq 0$$

$$P_{2im} = EI\omega k^3 |B_2^+| e^{-kx} (\cos kx - \sin kx), x \geq 0$$

For  $\alpha k$  very large then  $|A_2^+| = |A_1^-| = |B_1^-| = |B_2^+| = 1/\sqrt{2}$ . Also  $\phi_{A_1+B_1^-} = \pi/4$ ,  $\phi_{A_2+B_2^+} = 0$  and  $\phi_{A_1-B_1^-} = \pi/2$ . This gives the reactive power on the incident side and the transmitted side as

$$P_{1im} = 0.5 EI\omega k^3 e^{kx} (-\cos kx - \sin kx), x \leq 0$$

$$P_{2im} = 0.5 EI\omega k^3 e^{-kx} (\cos kx - \sin kx), x \geq 0$$

Which is the same form as the previous case.

The reactive power, normalised to the constant term in each case is plotted in Figure 3. There is a discontinuity in the reactive power at the crack. The magnitude of the peak level either side of the crack is equal, but there is a reversal of the sign at the crack. The reactive power damps out quickly reducing to zero for  $kx > 5$ .

## MEASUREMENT OF STRUCTURAL INTENSITY AND WAVE NUMBER

The wave decomposition method is well suited to intensity measurements in wave guides, such as beams and rods, Causse and Trolle [1988]. For the general case of two near-field and two far-field components in a beam four independent transducer measurements are required. Where there is only a single near-field component only three transducer measurements are required. It is not necessary to apply the finite difference correction, which is required for normal multi-transducer finite difference measurements, so the transducer spacing can be optimised for a particular measuring setup.

Measuring the acceleration, velocity or displacement at  $n$  locations on a beam gives  $n$  measurements of the form

$$w_i = A^+ e^{-jkx_i} + A^- e^{jkx_i} + B^+ e^{-kx_i} + B^- e^{kx_i} \quad i = 1, 2, \dots, n \quad (8)$$

where  $x_i$  is the location of the  $i$ th measurement. Equation (8) can be rewritten in matrix form as

$$\{W\} = [G] \{A\} \quad (9)$$

When the number of measurement locations equals the number of wave components then equation (9) can be rewritten as

$$\{A\} = [G]^{-1} \{W\} \quad (10)$$

For four measurement locations

$$[G] = \begin{bmatrix} e^{-jkx_1} & e^{jkx_1} & e^{-kx_1} & e^{kx_1} \\ e^{-jkx_2} & e^{jkx_2} & e^{-kx_2} & e^{kx_2} \\ e^{-jkx_3} & e^{jkx_3} & e^{-kx_3} & e^{kx_3} \\ e^{-jkx_4} & e^{jkx_4} & e^{-kx_4} & e^{kx_4} \end{bmatrix} \quad (11)$$

$$\{W\}^T = [w_1 \ w_2 \ w_3 \ w_4]$$

The active and reactive intensity may then be calculated from equations (5) and (7).

In addition to intensity measurement it was decided to make measurements of the local wavenumber  $k$  along the beam. The wavenumber,  $k$ , may be measured using three equi-spaced accelerometers. Using the finite difference approximations the measured value of  $k$  is given by, Wagstaff et al [1990],

$$k_{meas} = \frac{1}{\Delta} \sqrt{2 - H_{23} - H_{21}} \quad (12)$$

where  $H_{23}$  is the frequency response function between the second and third transducers and  $H_{21}$  is the frequency response function between the second and first transducers. The result must be corrected for the finite difference errors using the relation

$$k_{actual} = \frac{2}{\Delta} \sin^{-1} \frac{k_{meas} \Delta}{2} \quad (13)$$

thus

$$k_{actual} = \frac{2}{\Delta} \sin^{-1} \left( \frac{1}{2} \sqrt{2 - H_{23} - H_{21}} \right) \quad (14)$$

## INFINITE BEAM APPARATUS

The beam apparatus was constructed from a 6m long steel bar, with a cross-section 50mm x 5 mm, suspended by piano wire at four points and with each end embedded in conical shaped sand boxes to approximate anechoic terminations. The exposed length of beam for available for measurements was 5 m, Figure 4.

The beam was excited in the centre by a Gearing and Watson electro-magnetic shaker driving through a 2 mm diameter stainless steel stinger and a Bruel and Kjaer Type 8200 force transducer. Acceleration measurements were made with Bruel and Kjaer Type 4374 accelerometers, and Bruel and Kjaer Type 2635 charge amplifiers were used to condition all signals. Data were measured using a Hewlett Packard 3566A multi-channel analyser.

Cracks were simulated by cutting fine slots, approximately 1mm wide, in the beam with a thin slitting saw. Measurements of the active power and wave number along the beam in the region of the crack were made, for two cracks, one 0.8mm deep and the other 1.25mm deep. These represented values of  $\gamma$  of 0.3 and 0.5 respectively.

The variation of the wave number for the two cracks is shown in Figure 5. There is a clearly observable hump in the wave number measurements in the vicinity of the two cracks. The increase in wave number was observed when the three transducer array straddled the crack. This is because one of the transducers was then measuring the response of a different wave field from the other two.

In determining the wave components from the measurements, the origin of the near field waves was taken to be the crack location. Once the wave components had been determined the power at different points along the beam close to the crack were calculated. The magnitudes of  $k\alpha$  for the two cracks, over the frequency range tested, varied from a minimum of 0.02 to a maximum of 0.2. The maximum value of the reactive power is expected to be approximately 5% of the net incident active power. The expected magnitudes of the near field and the reflected wave components can be calculated from equation (4). The magnitudes of the experimentally measured values of the near field and reflected wave components were approximately equal, as predicted by equation (4), but the values were about double the theoretical values. The phase of the near field and reflected wave components were also larger than predicted by equation (4).

The reactive power, normalised with respect to the net incident active power, is shown in Figure 6 for different wave numbers. The curves clearly show the discontinuity in the reactive power at the crack, but the maximum values of the reactive power are approximately three times greater than expected. It can be seen that the magnitude of the reactive power at the crack site increases as the depth of the crack and the wave number increase.

The cuts used to represent the cracks were relatively wide with respect to their depth, because of the thin beam being used. As an alternative to the fracture hinge, the crack was modelled as a relatively short discontinuity, 1mm, with a reduced bending stiffness, Horner. Theoretical analysis for this model showed a reversal of sign in the reactive power at the discontinuity, similar to that observed for a crack. The magnitudes of the wave components and the peak values of the reactive power predicted using this model were about 20% higher than the measured values. The magnitude of the reactive power either end of the section was equal, as predicted by the theory.

## CONCLUSIONS

For a crack in a beam there is a sharp discontinuity in the reactive power at the crack site. The measurement of the reactive power has been shown to be a possible identifier of damage, as was the measurement of variations in the local wave number. For a lossless crack, where there is no localised increase in the damping, the wave number has been shown to be a superior indicator of local damage. The discontinuity in the reactive power is not as sensitive an indicator as a wave number measurement made with the transducer array straddling the crack.

## REFERENCES

Ju F.D., Akgun M., Wong E.T. and Lopez T.L., 1982, *Modal Method in Diagnosis of Fracture Damage in Simple Structures*, ASME Winter Meeting- Productive Applications of Mechanical Vibration, ASME, pp 113-126

Causse A. and Trolle J.L., 1988, *Dynamic Analysis of Nuclear Plant Circuit by Vibrational Intensity Measurement*, Proc. of Inter-Noise 88, Avignon, pp 579-582

Wagstaff P.R., Bouizem B. and Henrio J.C., 1990, *Optimization of Structural Intensity Measurements for Lightly Damped Structures*, 3rd Int Cong on Intensity Techniques, Senlis, 27-29 August, pp 257-264

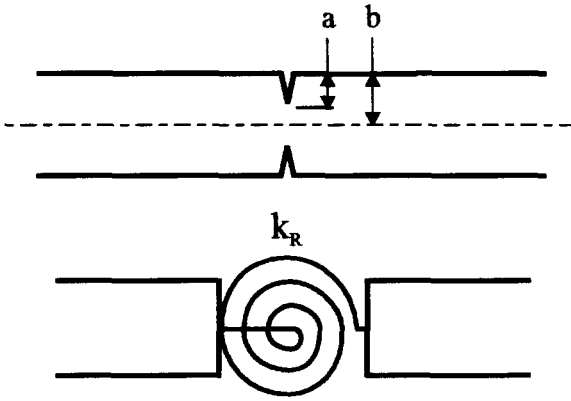


Figure 1 Fracture hinge representation of a crack.

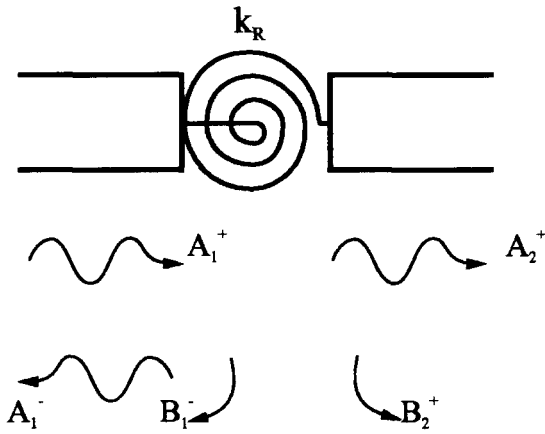


Figure 2 Incident reflected and transmitted flexural waves at crack.

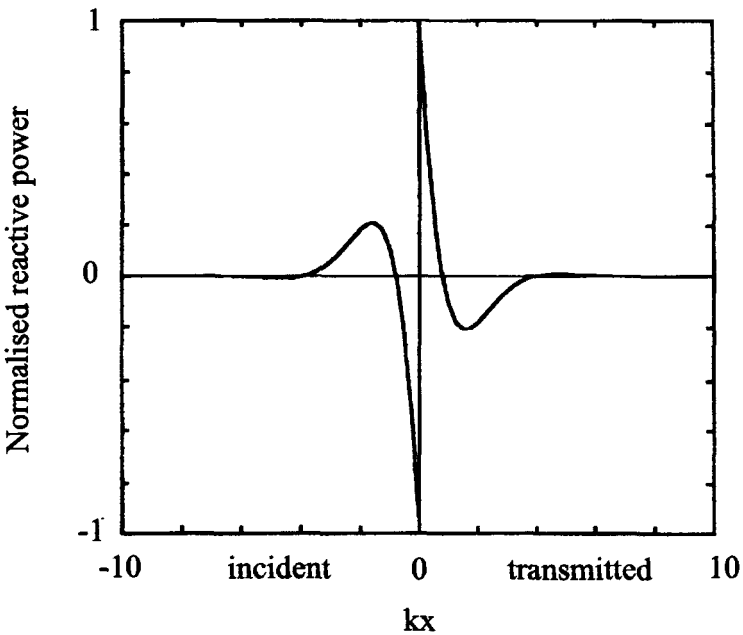


Figure 3 Normalised reactive power at a crack .

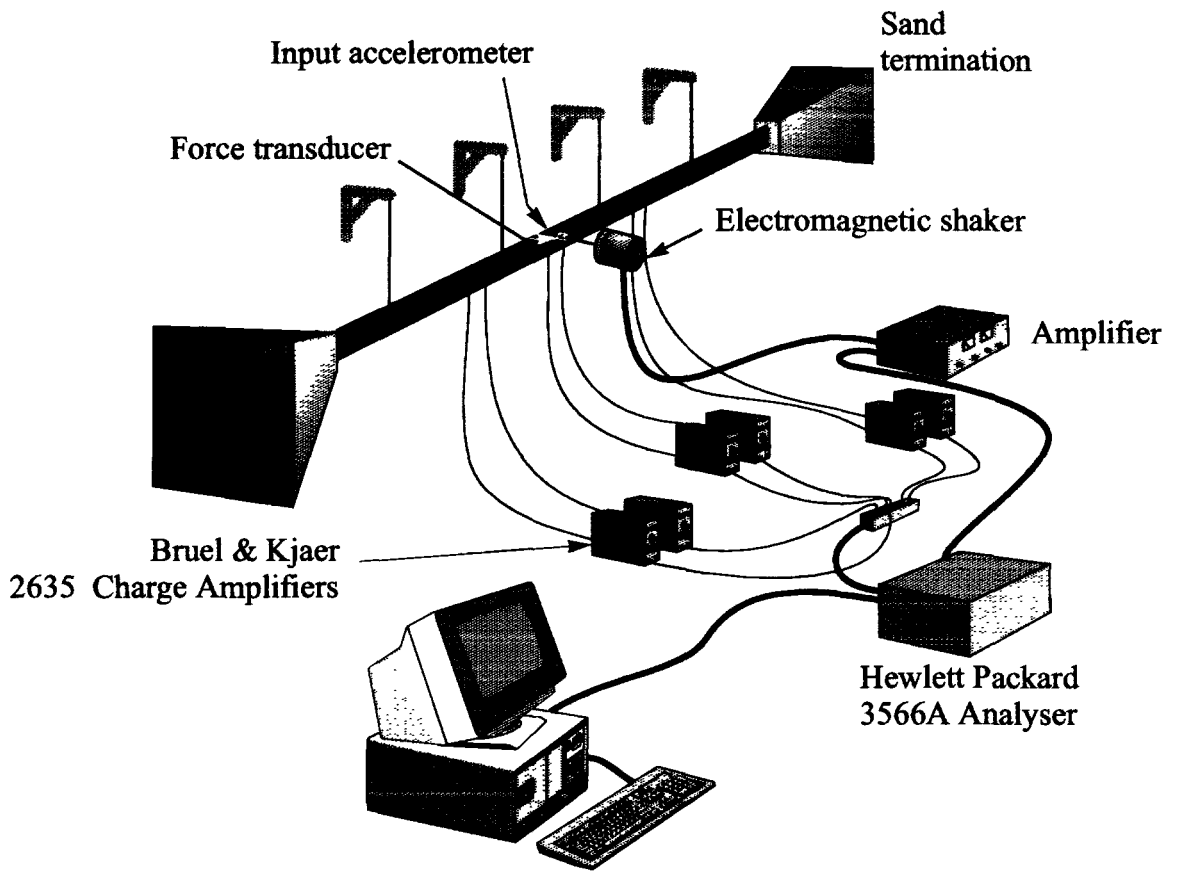


Figure 4 Schematic of beam apparatus and instrumentation.

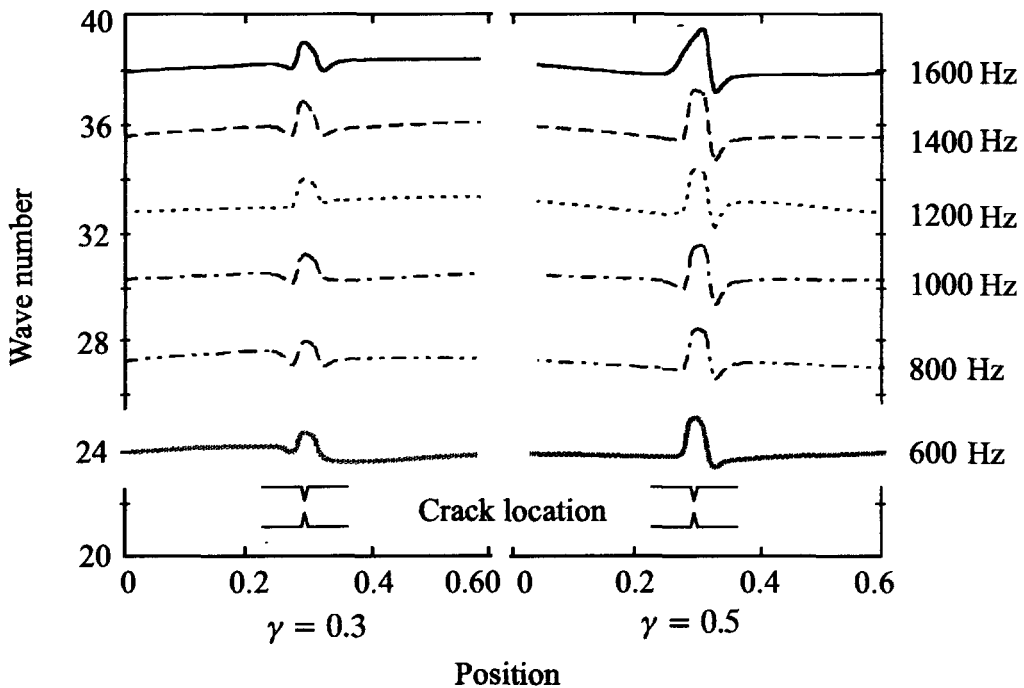


Figure 5 Variation in wave number in an infinite beam with a crack.

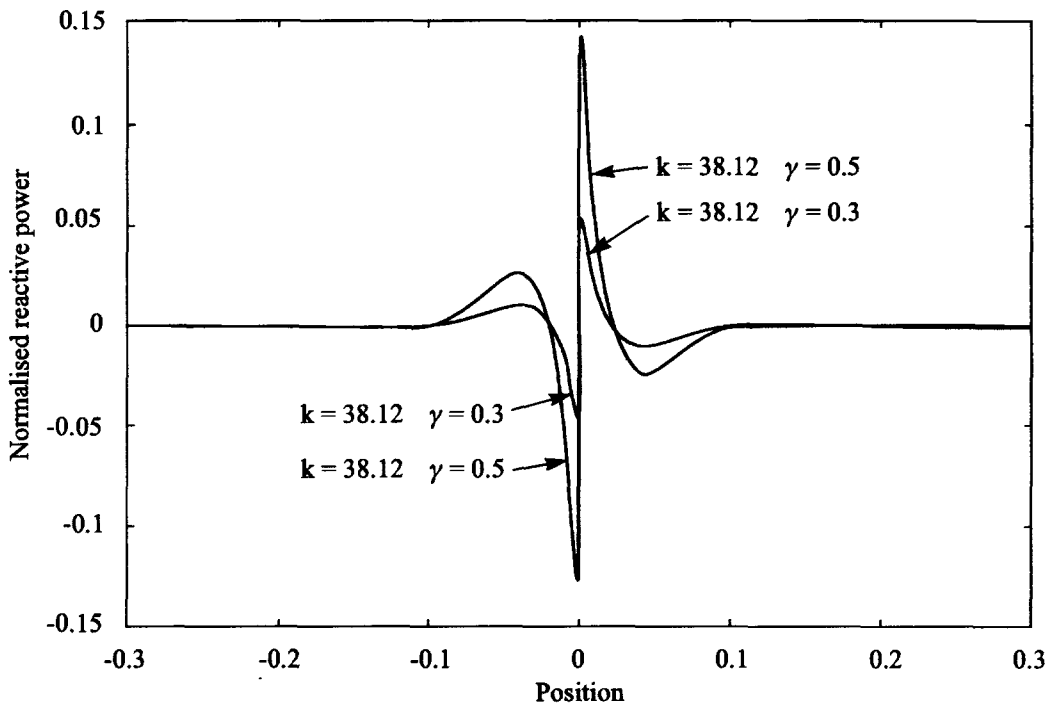
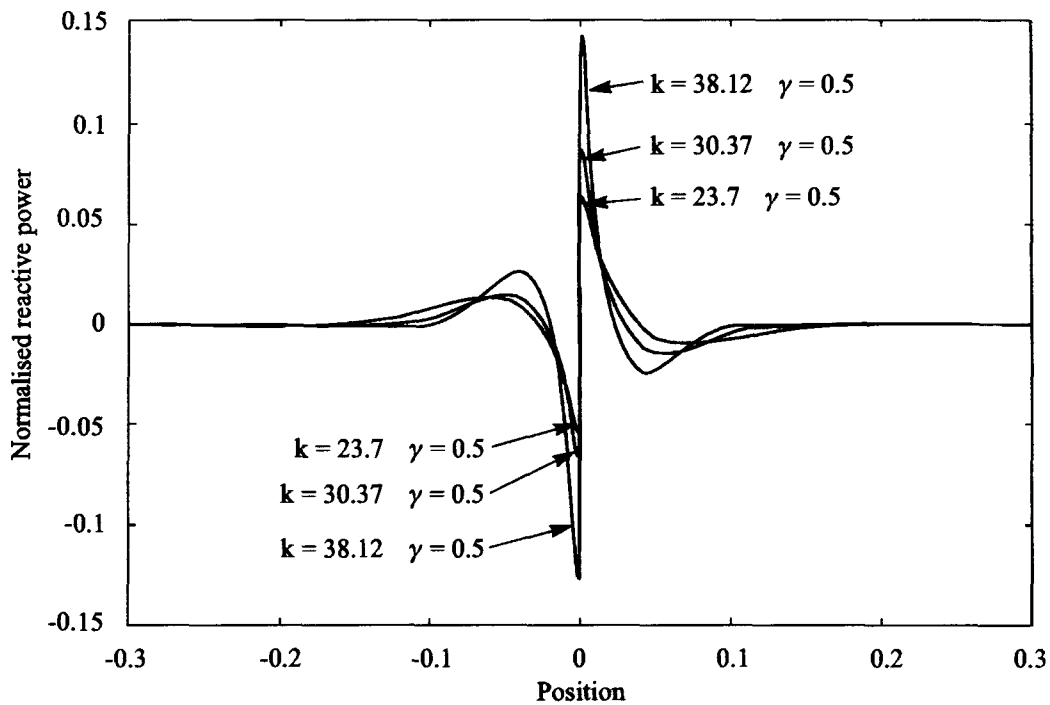


Figure 6 Experimental measurements of reactive power in a cracked infinite beam.